

# Integrating Additive Manufacturing and Repair Strategies of Aeroengine Components in the Computational Multidisciplinary Engineering Design Process

Khalil Al Handawi <sup>1</sup>, Lydia Lawand <sup>1</sup>, Petter Andersson <sup>2</sup>, Rebecka Brommesson <sup>2</sup>, Ola Isaksson <sup>3</sup>, Michael Kokkolaras <sup>1,3</sup>

<sup>1</sup>*Department of Mechanical Engineering, McGill University*  
*khalil.alhandawi@mail.mcgill.ca; lydia.lawand@mail.mcgill.ca;*  
*michael.kokkolaras@mcgill.ca*

<sup>2</sup>*GKN Aerospace Engine Systems Sweden*  
*petter.andersson@gknaerospace.com; rebecka.brommesson@gknaerospace.com*  
<sup>3</sup>*Department of Industrial and Materials Science, Chalmers University of Technology*  
*ola.isaksson@chalmers.se*

## Abstract

This paper presents a methodology for integrating failure and lifecycle analysis related to additive manufacturing in a computational multidisciplinary engineering design framework. The specific goal of this framework is to quantify the impact of component design decisions on system-level performance in order to assess alternative manufacturing, re-manufacturing and repair strategies from both technical and business perspectives. The ultimate objective of this research is to enable such considerations in the early product design phases, where sufficient degree of freedom exists to identify component design solutions that can facilitate and accommodate different manufacturing and repair techniques that impact the entire lifecycle. The developed methodology is demonstrated by means of a jet engine component where repair strategies are included as variables in the computational design process. Numerical results confirm that these strategies can be used to trade among design attributes such as lifecycle cost, weight, and performance.

**Keywords:** *Additive Manufacturing, Multidisciplinary Design Optimization, Aeroengine Components, Repair and Remanufacturing, Structural Analysis, Lifecycle Cost*

## 1 Introduction

As a manufacturer of aeroengine components, GKN Aerospace Engine Systems Sweden acts both as a supplier and a customer within the supply chain. Therefore, it needs to develop scalable models that can support fast and quantitative analysis, design and optimization studies of components to assess system-level performance, manufacturability, and cost within the envelope of a product platform. Knowledge-based engineering rules are used for automated geometry generation, which enables swift construction of hundreds of parametric models. These are then used to create computational models for several types of analysis: structural, aerodynamics, tolerance analysis, manufacturing simulation, and cost. Computational designs of experiments are conducted to identify the variables that are most important for different properties such as mechanical strength and manufacturability. The obtained analysis results can also be used to build response surfaces for efficient surrogate-assisted optimization.

In this paper, we consider additive manufacturing as an alternative for remanufacturing or repairing a component, develop models for related performance and lifecycle cost analysis, and integrate them into the computational design optimization process. Since design is a complex activity, involving artifacts, people, tools, processes, organizations and the environment in which this takes place, we adopt the design research methodology (DRM) approach presented in ([Blessing & Chakrabarti, 2009](#)). The main stages of the DRM include criteria definition stage which identifies the aim of the research project, the descriptive study stage which identifies factors that influence the formulated criteria and act as a basis for the development of support to improve the design and the prescriptive study stage which develops impact models describing the expected improved situation. In this spirit, our design study process is conducted on a case study involving multidisciplinary analysis of a turbine rear structure (TRS); a structural load bearing component of an aero-engine. The interaction of different loads and disciplines makes the design of such a component an interesting problem from an optimization perspective. The approach is not to design from scratch but rather re-design an existing component with a reinforced structure by means of additive manufacturing (AM) techniques. This structural reinforcement is accomplished through a circumferential stiffener added to the outer casing of the TRS. The key dimensions (and design variables) of this geometrical configuration are outlined in Figure 1.

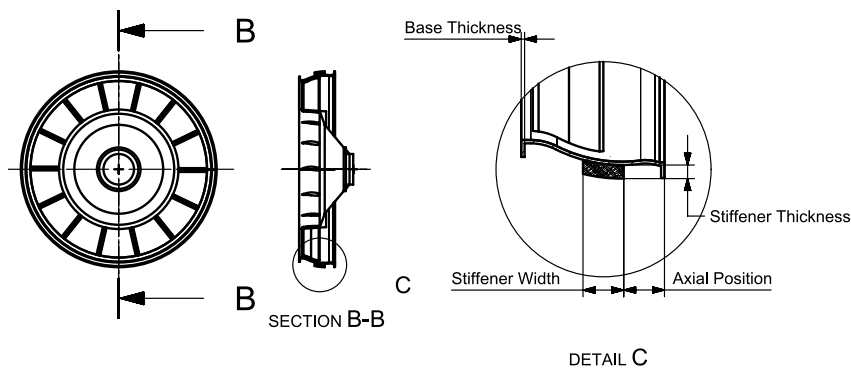


**Figure 1. Geometry governing the stiffener design problem (represented by the hatched area in Detail C)**

The multidisciplinary analysis environment will be developed for the described case study with two main disciplines in mind; Structural performance of the TRS and the alteration of its lifecycle costs. The following session describes the methodology that was undertaken.

## 1.1 Methodology

We first formulate and solve a bi-objective optimization problem related to structural considerations. We then build and integrate a lifecycle cost (LCC) model to formulate and solve a single-objective optimization in order to obtain a single design that yields minimized lifecycle cost. The whole analysis process is automated. The necessary steps to of this process are outlined in detail below:

1. Geometry and model setup: The geometry design variables and parameters are used to generate the associated computer-aided design (CAD) model. Other parameters are used in subsequent analysis within each discipline (load cases, material selection, etc.). The geometry is meshed (mesh size is also a design parameter) and loads are applied to initialize the structural analysis. Appropriate geometry information is also extracted to be used in the LCC sub-model. Specifics of the analysis are given in Section 2.
2. The two disciplines are run simultaneously with any associated interactions to arrive at a number of output variables. All output variables (both intermediate and final outputs) are tabulated and stored for subsequent design space visualization.
3. Design variables are sampled equally and all associated output variables with each design are tabulated. The 4-dimensional design space is visualized using combinations of two-dimensional projection plots: All 6 possible combinations are plotted side by side to visualize the impact of each variable on the design objective.

## 2 Structural Considerations

For the purpose of this case study, a direct energy deposition (DED) process is used to redesign the TRS outer casing to improve its structural performance. However, the DED process employs an energy source to increase the temperature of the raw and parent material such that they exceed the melting temperature of either constituent material (Debroy et al., 2018). For the sake of simplicity, both constituents will be assumed to be the same material. Furthermore, the energy supplied will be modeled as a heat flux incident on the build surface which is a simplification of the heat transfer process from the DED tool to the part (TRS). Furthermore, heat is naturally convected from the part and no other cooling process is assumed.

### 2.1 Modelling Approach

The major outcome of the DED process are induced residual stresses in the structure which may have an impact on the fatigue and LCC models. As a subproblem, this discipline will be concerned with maximizing the factor of safety as a proxy of structural integrity subject to residual stresses on the component by manipulating the location and geometry of the deposited stiffener as well as DED process parameters. For simplicity of analysis, the DED process is simplified to a uniform heat flux applied at the surface of the stiffener geometry until steady state temperature is reached (Figure 3a). Afterwards, the structure is cooled by convection until steady state at which point the residual stress field is obtained (Figure 2).

The residual stress field is imported into a new analysis step where an internal pressure load is applied on the inside of the outer casing to simulate pressurizing the structure during service (Figure 3b). The new stress field is obtained and a cyclic loading failure analysis is performed to determine how many pressurization cycles the structure can withstand using the modified Goodman failure criterion.

Figure 4 shows the obtained stress field at the end of the heating (Figure 4a) and cooling phases (Figure 4b).

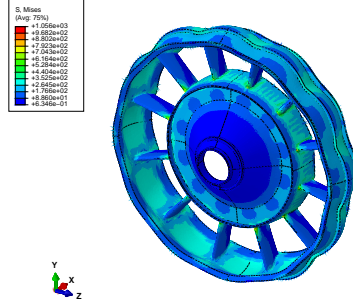


**Figure 2.** Example of residual stress field (MPa) after subjecting the stiffener and TRS to uniform heating followed by cooling in air

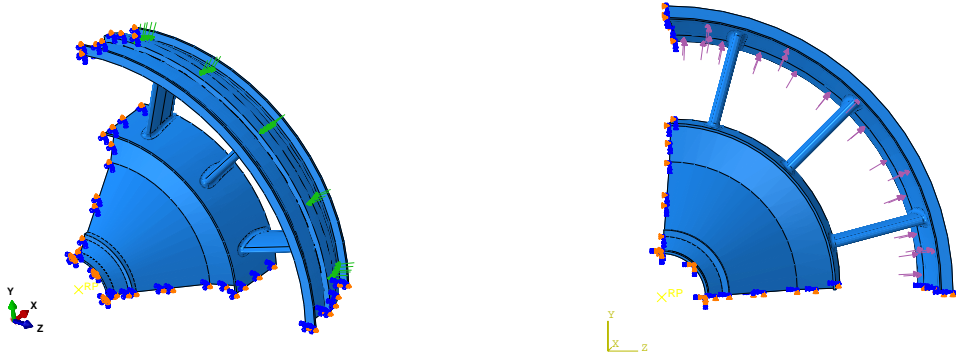


**Figure 3.** Problem setup of the two main analysis phases

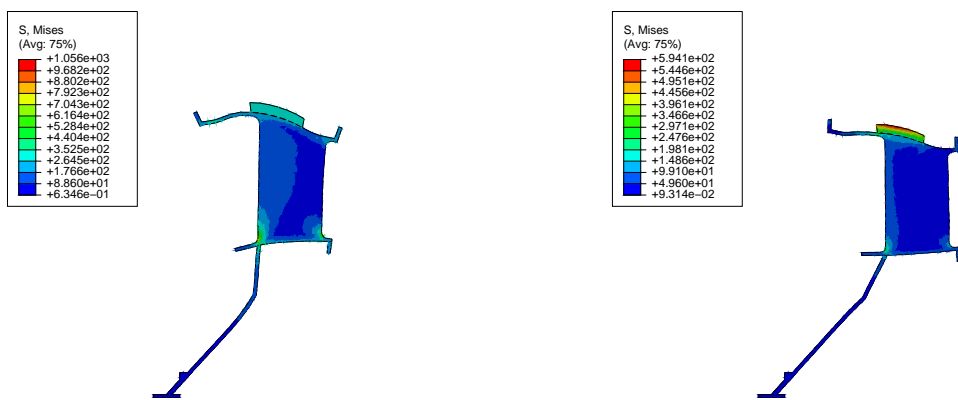


**Figure 4.** Cross sectional view through TRS struts showing the effect of heating and cooling on the TRS structure

## 2.2 Optimization

The design variables are listed in Table 1. The first three are geometry variables governing

**Table 1.** Design variables

Variable	Symbol	Units
Stiffener axial position	$x_1$	mm
Stiffener thickness	$x_2$	mm
Stiffener width	$x_3$	mm
Supplied thermal power of DED process	$h_{\text{flux}}$	W/mm <sup>2</sup>

the position, thickness, and width of the stiffener; the fourth one is a DED process parameter governing the energy supplied during the manufacturing process to heat the base material so that new material can be sintered on top. The objectives are to maximize safety factor as a proxy of structural integrity and minimizing weight. The constraints contain the stiffener within the limits of the existing design while ensuring sufficient discretization of the geometry to capture the thermoelastic behavior of the part. Furthermore, a lower bound is set on the temperature profile on the TRS in order to achieve melting of the deposited and parent materials. The multi-objective optimization problem formulation is

$$\begin{aligned} \underset{\mathbf{x}}{\text{minimize}} \quad & f_1(\mathbf{x}; \mathbf{p}_1) = -n_f \\ & f_2(\mathbf{x}; \mathbf{p}_2) = W_s \\ \text{where} \quad & \mathbf{x}^T = [x_1, x_2, x_3, h_{flux}] \end{aligned}$$

subject to

$$\begin{aligned} g_1(\mathbf{x}) &= x_3 + x_1 - W_{\text{total}} \leq 0 \text{ (geometric constraint)} \\ g_2(\mathbf{x}) &= T_m - T(x_1, x_2, x_3, h_{flux}, T_{\text{ambient}}, K_m, h_{\text{conv}}) \leq 0 \text{ (achieve melting requirement)} \\ b_1(\mathbf{x}) &= A_{xi} + 2 \leq x_1 \leq W_{\text{total}} - 2m_s \text{ (computational model constraint)} \\ b_2(\mathbf{x}) &= t_{\min} \leq x_2 \leq t_{\max} \text{ (computational model constraint)} \\ b_3(\mathbf{x}) &= m_s \leq x_3 \leq 120 - 2m_s \text{ (geometric constraint)} \\ b_4(\mathbf{x}) &= 0.07 \leq h_{flux} \leq 0.25 \text{ (process constraint)} \end{aligned}$$

The design parameters contained in the vectors  $\mathbf{p}_1$  and  $\mathbf{p}_2$  are listed in Table 2.

**Table 2. Design parameters used in DED process simulation subsystem**

Parameter	Symbol	Value	Units
Material Young's Modulus	$E_m$	204	GPa
Material thermal conductivity	$K_m$	11.4	W/m·K
Material coefficient of thermal expansion	$\alpha_m$	$1.3 \times 10^{-5}$	K <sup>-1</sup>
Initial axial position	$A_{xi}$	35	mm
Outer TRS case width	$W_{\text{total}}$	155	mm
Nominal FEA element size	$m_s$	13.75	mm
Ambient temperature	$T_{\text{ambient}}$	23	°C
Convection heat transfer coefficient	$h_{\text{conv}}$	20	W/m <sup>2</sup> ·K
Minimum stiffener thickness	$t_{\min}$	5	mm
Maximum stiffener thickness	$t_{\max}$	25	mm
Material melting temperature	$T_m$	1200	°C
Density of stiffener material	$\rho$	8190	g/cm <sup>3</sup>
Internal Pressure	$P_i$	-4	MPa
Fatigue Notch factor	$Kf_1$	1.9	
Number of load occurrences per cycle	$n_1$	2	
Material yield stress	$\sigma_{ym}$	1110	MPa
Material ultimate strength	$S_u$	1304	MPa

Solving the optimization problem showed that maximizing  $h_{flux}$  would bring about a maximization in  $n_f$  (Figure 5a). As a result, the upper limit of the box constraint  $b_4$  is likely to be active. Furthermore, the two variables  $x_1, x_3$  are both monotonic with respect to  $n_f$  and as a result,

the linear constraint  $g_1$  is also likely to be active. This result indicates that significant thermal deformation of the structure is likely to improve the safety factor against fatigue due to the compressive nature of the stresses at the foot of the struts (Figure 4b). Being in a compressive region of cyclic loading, the structure is likely to be more resilient against fatigue crack propagation of any likely defects in that area. However, the remaining two variables,  $x_2$  and  $x_1 = (155 - x_3)$ , are likely to be non-monotonic with respect to  $n_f$ . This is evident from Figure 5 which shows this non-monotonicity for axial position ( $x_1$ ) and thickness ( $x_2$ ).

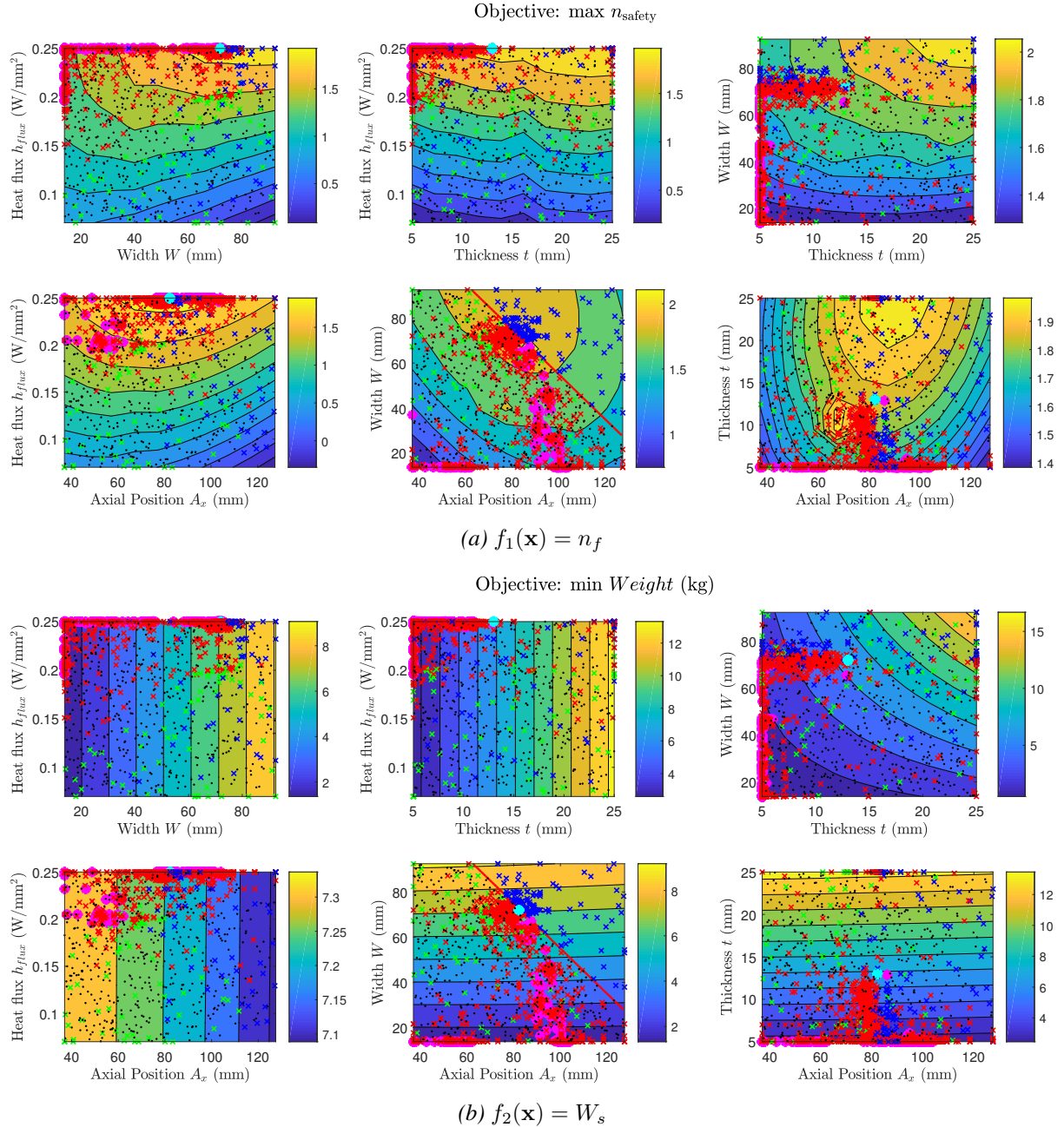


**Figure 5.** Points evaluated during design space exploration by NOMAD: ( $\times$ ); Pareto-optimal points: ( $*$ ); infeasible points: ( $\times$ ); invalid points: ( $\times$ ); initial guess: ( $*$ )

Comparing Figures 5a and 5b show an interesting competition between the two objectives (a classical structural design trade-off problem). NOMAD's bi-objective features were used to solve such a problem. Figure 5 shows the iterations towards the Pareto frontier. Note that invalid points are encountered where the model crashed due to violation of the physical constraint

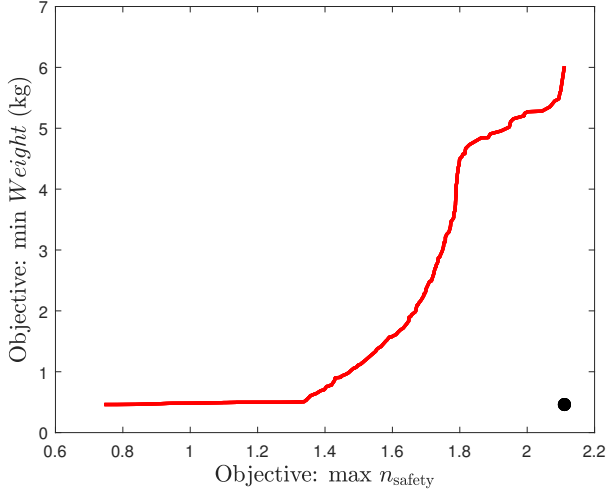


**Figure 6.** Pareto front constructed using SAO between  $f_1$  and  $f_2$  showing a nonconvex attainable set

( $g_1$ ). Direct black box evaluations were avoided for the purpose of this study due to their high computational cost. As a result, a Kriging surrogate model was used instead of the blackbox. This is known as surrogate-assisted optimization (SAO).

The final result of this study is shown graphically in Figure 6. It can be seen that the attainable set is nonconvex which implies that weighting methods for evaluating a combined objective would fail for such a case.

### 3 Lifecycle cost considerations

This section focuses on calculating the costs of manufacturing the stiffener using DED as well as its effect on the lifing decisions of the whole TRS. In order to properly assess lifecycle costs, the whole product lifecycle needs to be considered, from the first idea until the final disposal of the part. An analytical function that calculates the total cost for the different design variables was developed and used. Then an overall optimization model on the whole system, both structural and LCC model, was performed to study the correlation between different objectives that is needed to reach an optimum solution. Further assumptions were made throughout the LCC analysis process in order to simplify the model and make it suitable for our particular application. These assumptions include:

- Costs are calculated for a single part production per build
- Only DED technique is taken into consideration
- Only one laser is used
- Deposited layer thickness is fixed throughout the AM process
- Costs of the inert gas used are neglected
- TRS surface preparation is not considered
- Post processing costs are not considered
- Recycling or disposal stage is not considered
- Operator's hourly rate is assumed constant for all processes

#### 3.1 Modelling approach

Like any other AM technique, lifecycle of DED starts with preparing the geometric data, assembling the build job, setting up the machine, building the part and finally removing it from the machine (disassembly). Costs involved in each of these stages are calculated using a time-driven activity based costing model ([Lindemann, Jahnke, Moi, & Koch, 2013](#); [Fera, Fruggiero,](#)

Costabile, & Pham, 2017; Thomsen, Kokkolaras, Måansson, & Isaksson, 2016). Further costs for repairing and replacing the TRS module are taken into consideration as well. Equation 1 shows the overall modelling equation used to calculate the total cost that accounts for all the stages involved in the LCC analysis. Main factors associated with the costs of each stage include build time, amount of energy consumed, labor wages, build part dimensions, fatigue life of the part, process speed and other process parameters.

$$C_{\text{Total}} = C_{\text{Prep}} + C_{\text{build job}} + C_{\text{setup}} + C_{\text{build}} + C_{\text{removal}} + C_{\text{repair}} \quad (1)$$

### 3.2 Integrated optimization problem

The outputs of the DED process model presented earlier (Section 2) were used as inputs for the LCC model, on which an integrated optimization problem was solved. Optimization process helps identify the optimal solution for the problem under study which is of great use for many sectors especially those that require decision making. The hierarchy of the overall problem is shown in Figure 7. It should be noted that Figure 7 highlights the distinction between the

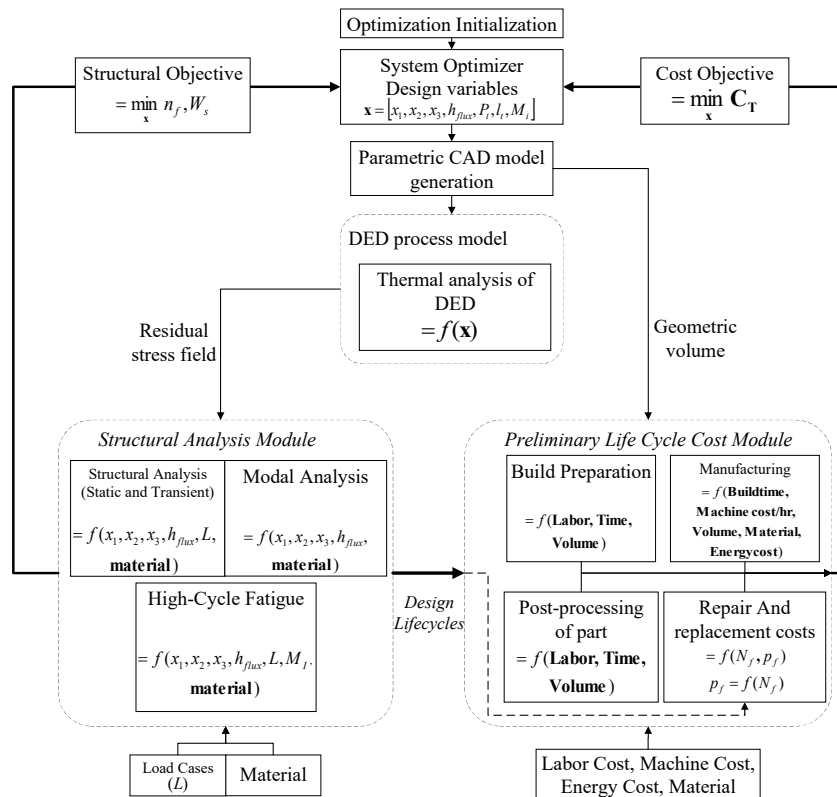


**Figure 7. Outline of proposed system architecture**

optimization process and the analysis procedure. The integrated optimization problem features a single objective, namely to minimize the total cost.

$$\underset{\mathbf{x}}{\text{minimize}} \quad f(\mathbf{x}; \mathbf{p}_3) = C_{\text{Total}}$$

$$\text{where} \quad \mathbf{x}^T = [x_1, x_2, x_3, h_{\text{flux}}]$$

subject to

$$\begin{aligned}
g_1(\mathbf{x}) &= x_3 + x_1 - W_{\text{total}} \leq 0 \text{ (geometric constraint)} \\
g_2(\mathbf{x}) &= T_m - T(x_1, x_2, x_3, h_{\text{flux}}, T_{\text{ambient}}, K_m, h_{\text{conv}}) \leq 0 \text{ (achieve melting requirement)} \\
b_1(\mathbf{x}) &= A_{xi} + 2 \leq x_1 \leq W_{\text{total}} - 2m_s \text{ (computational model constraint)} \\
b_2(\mathbf{x}) &= t_{\min} \leq x_2 \leq t_{\max} \text{ (computational model constraint)} \\
b_3(\mathbf{x}) &= m_s \leq x_3 \leq 120 - 2m_s \text{ (geometric constraint)} \\
b_4(\mathbf{x}) &= 0.07 \leq h_{\text{flux}} \leq 0.25 \text{ (process constraint)}
\end{aligned}$$

The design parameters contained in the vector  $\mathbf{p}_3$  are listed in Table 3.

The model described in Section 2.1 turns out to be computationally intensive due to the coupling of the displacements and temperatures during each transient step. The model will now be termed a “Blackbox” that accepts the design variables as an input ( $\mathbf{x} = x_1, x_2, x_3, h_{\text{flux}}$ ) and outputs the objective ( $f(\mathbf{x}) = C_{\text{Total}}$ ) and the nonlinear constraint ( $g_2(\mathbf{x}) = T_m - T$ ). A direct search algorithm (mesh adaptive direct search (MADS)) with good convergence properties is required for this highly nonlinear problem. For the purpose of this discussion, the NOMAD implementation of MADS was used and no other algorithms were used due to huge amount of computational time required to obtain a single optimization result. Again, direct black box evaluations were avoided for the purpose of this study and a Kriging surrogate model was used instead of the blackbox.

It can be clearly seen that maximizing  $h_{\text{flux}}$  would bring about a minimization in  $C_{\text{Total}}$  (Figure 8). Optimization results showed that there is a strong dependency of the optimum on initial guess. A better initial for the same algorithmic parameters, reduces the required number of blackbox evaluations. Furthermore, it was observed that the direction type chosen, mesh size used and maximum allowed number of blackbox evaluations all have an effect on the optimum solution obtained. Table 4 displays the best result among the obtained optima from the LCC model and also displays the corresponding weight and safety factor for subsequent discussions.

Accurate cost analysis relies on quality of data which is a challenging issue associated with LCC calculations. In particular, results are heavily dependent on future trends for economic data and the corresponding uncertainty (i.e. inflation rate and energy prices) especially when prediction are being made over a long period. Another uncertain area in LCC is determining the service life of a component which usually depends on other various analyses. This integrated frameworks presented in this paper is an iteration towards such a strategy by assimilating structural simulations and considerations within a simplified LCC model with more detailed models to be constructed on this basis in future iterations of this work.

## 4 Conclusions

This paper presents a design platform that can be adopted to match new design alternatives. A representative case study in the aerospace industry was chosen to demonstrate the capabilities of the developed analysis methodology. The multidisciplinary analysis environment was setup for the described case study with two main disciplines in mind; Structural performance of TRS and the alteration of lifecycle costs of the TRS. Integrating the DED process simulation model with the LCC model helped in visualizing trade-offs. The number of lifecycles of the model under study were obtained along with fatigue calculations and factor of safety from the structural model. These were then used to study their effect on the maintenance intervals and repair cost in the LCC model. Results clearly showed that configurations that maximize the surface area

**Table 3. Design parameters used in LCC model subsystem**

Parameter	Designation	Assumed Value	Unit
Pre-processing operators hourly rate	$C_{op}$	54	euros/hr
Hourly rate of the workstation including costs of required software and tools	$C_{pc}$	30	euros/hr
Time required for preparing CAD data	$T_{prep}$	1	hr
Time required for build job assembly	$T_{buildjob}$	1	hr
Time required for machine setup	$T_{setup}$	1	hr
Factor to model the frequency of material changes	$F_m$	0	
Time required to change material	$T_{mat}$	1	hr
Extra effort in handling protective gas environment	$F_{inert}$	1	
Fixed time consumption per build	$T_{job}$	1	hr
Fixed time consumption per layer	$T_{layer}$	0.003	hr
Layer thickness	$L_{thick}$	0.002	cm
Density of Inconel 718	$\rho_m$	8.192	$\text{Kg}/\text{m}^3$
Total indirect cost per machine hour	$C_{indirect}$	26.64	euros/hr
Mean price of electricity for the manufacturing sector in UK	$P_{energy}$	0.018	euros/MJ
Energy consumption per build job	$E_{job}$	57.6	MJ
Energy consumption per build and layer	$E_{layer}$	0.000013	MJ
Energy consumption rate	$E_{time}$	142.58	MJ
Energy attributable to the scanning of 1 $\text{mm}^2$ per build	$\beta_{time}$	0.000013	MJ
Mean energy cost	$C_{energy}$	0.21	euros/KWh
Utilization factor	$k_u$	0.8	
Waste factor for powder	$W_f$	1.1	
Material costs	$C_{material}$	107	euros/Kg
Number of flying cycles	$F$	20000	
Wiebull distribution coefficient	$k$	2	
Depreciation time	$D_t$	5	years
Machine uptime	$M_{uptime}$	30	
Factor to model extra effort required for handling in protective gas environment	$F_{inert}$	1	
Time required for removing parts from the machine chamber	$T_{removal}$	1	hr
TRS replacement cost	$C$	4,255.00	Euros

**Table 4. Values at LCC model optimum point**

Output	Value
Cost	1032 Euros
Weight	2.27 kg
Safety factor	1.75

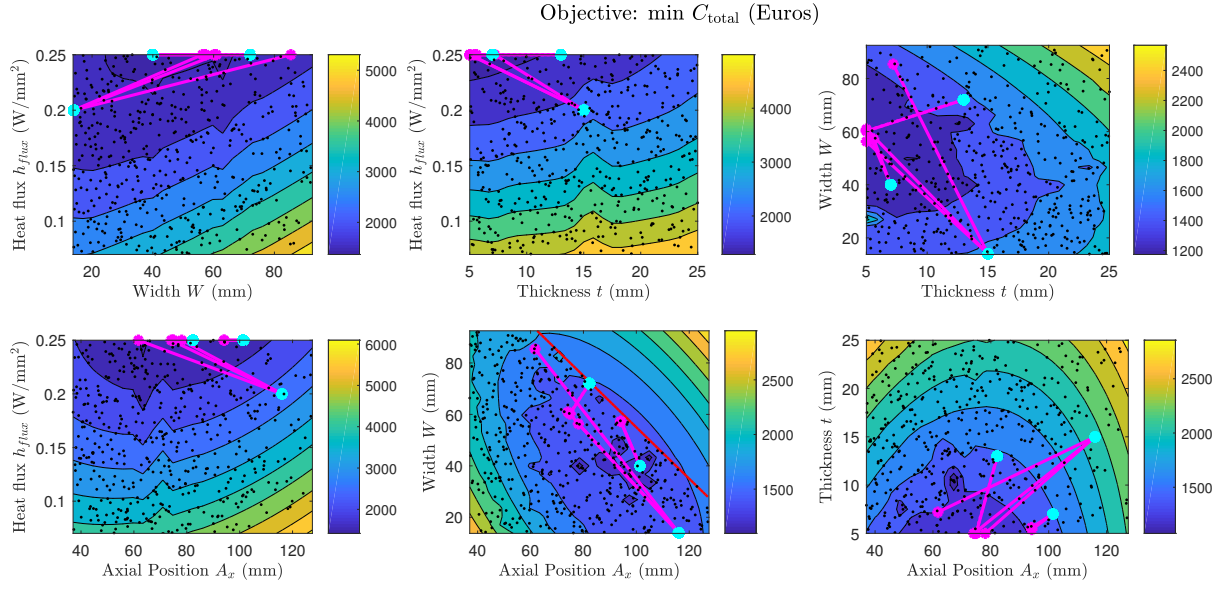


**Figure 8.** Kriging surrogate model constructed using LH sampling and progress of NOMAD towards optimum for different initial guesses; initial guess: (\*); Optimizer: (\*)

of the stiffener while reducing the amount of heat that can escape by convection are favorable from a design safety point of view. Moreover, an increase in the value of heat flux in the DED process caused an improvement in the component's structural performance which resulted in a decrease in the total cost value. Comparing results obtained from optimization of the structural model and the integrated LCC model (Table 5), the following conclusions can be drawn:

- The LCC model can be thought of as a criterion to assist the designer in selecting from among the Pareto optima (since the LCC optimum lies within the Pareto set Figure 9).
- LCC model optimum is incidentally closest to the point on the frontier that is also the closest to the utopia (Figure 9). Therefore, the point closest to the utopia obtained from structural considerations only, corresponds to minimum cost since the cost function decreases monotonically with weight and increases monotonically with safety factor.

In conclusion, there is relatively large agreement between the LCC model optimum point and the Pareto point that lies closest to the utopia Point. The reason for this is that the service life of the component predicted by the structural model seems to have the largest effect on the LCC model.

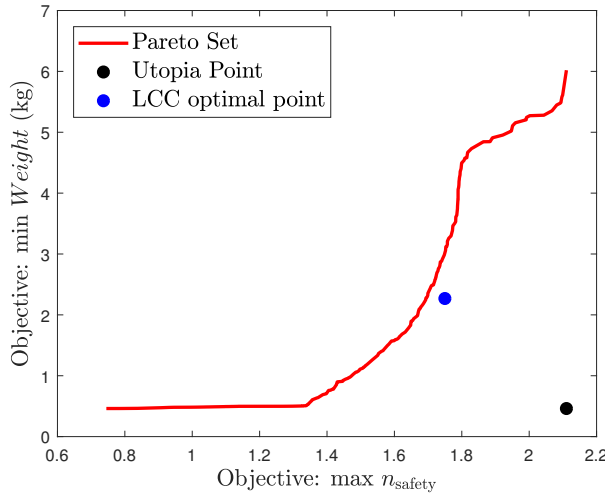


**Figure 9.** LCC optimum in comparison with Pareto frontier obtained from structural considerations

**Table 5.** Values of LCC optimum point and Pareto point closest to utopia in the structural model

Design Variables	LCC Optimum	Pareto point closest to utopia
Axial position (mm)	94.06	83.79
Thickness (mm)	5.60	5.02
Width (mm)	57.25	64.76
Heat flux ( $W/mm^2$ )	0.25	0.25

#### 4.1 Future Work

The established methodology is generic and will be used in subsequent design studies to establish an optimization toolbox. Higher fidelity models for structural analysis and LCC analysis of the part will be utilized. Furthermore, future directions could include incorporating a new sub-model to simulate the AM process itself and compute effect of thermal gradients on residual stresses and deflections. This will add an additional interaction with the LCC model as AM process parameters directly influence the build cost. Different optimization strategies could also be explored for developed analysis models (incorporated surrogate sub-models) along with the effect of relaxing some of the constraints on the optimal solutions. Finally, parametric analysis will be performed on the effect of thermal properties of the material assumed in this study.

#### Acknowledgements

The first two and the last authors are grateful for the partial support of their work by grants NSERC CRDPJ 479630-15 X-243027 and CARIC CRDPJ479630-15 X-243067. The work of the third and fourth effort has been partially supported by European Union's Horizon 2020 research and innovation programme under grant agreement No 690608. Such support does not constitute an endorsement of the opinions expressed in this paper.

#### References

- Blessing, L., & Chakrabarti, A. (2009). *DRM, A Design Research Methodology*. Springer.
- Debroy, T., Wei, H. L., Zuback, J. S., Mukherjee, T., Elmer, J. W., Milewski, J. O., ... Zhang, W. (2018). Additive Manufacturing of Metallic Components. *Progress in Materials Science*, 92, 112–224.

- Fera, M., Fruggiero, F., Costabile, G., & Pham, D. (2017). A New Mixed Production Cost Allocation Model for Additive Manufacturing (MiProCAMAM). *International Journal of Advanced Manufacturing Technology*, 92(9-12), 4275–4291. doi: 10.1007/s00170-017-0492-x
- Lindemann, C., Jahnke, U., Moi, M., & Koch, R. (2013). Impact and Influence Factors of Additive Manufacturing on Product Lifecycle Costs. In *Proceedings of the 24th Solid Freeform Fabrication Symposium* (pp. 998–1009).
- Thomsen, B., Kokkolaras, M., Måansson, T., & Isaksson, O. (2016). Quantitative Assessment of the Impact of Alternative Manufacturing Methods on Aeroengine Component Lifing Decisions. *ASME Journal of Mechanical Design*, 139(2). doi: 10.1115/1.4034883